De Novo Design, Synthesis, and Evaluation of Novel Nonsteroidal Phenanthrene Ligands for the Estrogen Receptor

Jonathan M. Schmidt,[†] Julie Mercure,[†,‡] Gilles B. Tremblay,[§] Martine Pagé,[§] Aida Kalbakji,[§] Miklos Feher,[†] Robert Dunn-Dufault,[†] Markus G. Peter,[†] and Peter R. Redden*,[†]

SignalGene Inc., 335 Laird Road, Unit 2, Guelph, Ontario, Canada N1G 4T2, and SignalGene Inc., 8475 Avenue Christophe-Colomb, bureau 1000, Montreal, Quebec, Canada H2M 2N9

Although there are many estrogen receptor antagonists with improved tissue selectivity profiles compared with tamoxifen, optimal tissue selectivity has not yet been demonstrated. As such there is still a need for additional diversity and new chemical scaffolds to allow for exploration of improved tissue selectivity. Here, we describe the discovery of a novel phenanthrene scaffold for estrogen receptor ligands utilizing a ligand based de novo design approach. The nanomolar binding of phenanthrenes, **12b**,**c**, **14b**,**c**, and **15** against human recombinant ER_α indicates that our ligand based de novo design approach was successful. From a gene transfection assay, **12b**,**c**, **14b**,**c**, and **15** displayed only antagonistic activity with no observable agonistic activity. The alkyl 9,10-dihydrophenanthrene **16** (presumably a racemic mixture) was a substantially more potent ER binder than the phenanthrenes. It also displayed only antagonistic activity and was effective at inhibiting estradiol stimulated MCF-7 cell proliferation. These results demonstrate that this phenanthrene (and 9,10-dihydrophenanthrene) scaffold warrants further study as potential selective estrogen receptor modulators and/or pure antiestrogens.

Introduction

Estrogen receptors (ER) are members of a superfamily of ligand-activated transcription factors, which includes progesterone, androgen, and glucocorticoid and mineralocorticoid receptors, as well as receptors for thyroid hormone, retinoids, and vitamin D.[1] Additionally a large group of receptors known as 'orphan receptors', for which no ligand has been described, belong to this superfamily.

Stimulation of estrogen receptors by endogenous estrogens plays an important role in both male and female physiology. Estrogens are involved in the regulation of cholesterol and lipid levels, the skeletal system, the central nervous system, and reproductive functions.[2,3] However, estrogen stimulation is also implicated in the development of breast cancer.[4] Consequently, many estrogen receptor ligands (see Figure 1) are being developed with the aim of preventing estrogen-mediated tumor growth. Tamoxifen, which was originally developed as an estrogen receptor antagonist, is currently the hormonal treatment of choice for both pre- and postmenopausal women with breast carcinoma. It is now known that tamoxifen and other selective estrogen receptor modulators (SERMs) display a broad range of agonist and antagonist activity dependent on the tissue and species being evaluated and that several factors are thought to contribute to this phenomenon.[5−8] Recently, a new estrogen receptor subtype was discovered and designated ER_β.[9] Experiments based on the tissue distribution and pharmacology of ER_α and ER_β
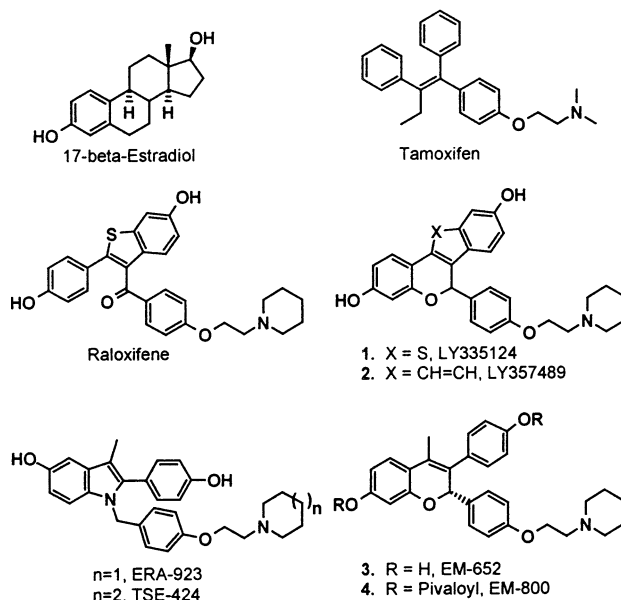

Figure 1. Estrogen receptor ligand structures.

suggest that the tissue selectivity of certain estrogens may be related, at least in part, to their different effects at the ER_α and ER_β subtypes.[7,10,11] Other factors that may contribute to selectivity include the tissue-specific presence of corepressors and coactivators, and the cell/tissue/species accessibility of different DNA-response elements.[8,12]

Since the tissue selective effects of tamoxifen have been discovered, other SERMs with improved selectivity profiles have been or are being developed (Figure 1). These include the benzothiophenes[7,13,14] (raloxifene and related analogues **1**, LY335124 and **2**, LY357489) and triphenylethylene analogues[7,15,16] (including tamoxifen),

---

* To whom correspondence should be addressed: Tel (519)-823-9088. Fax (519)-823-9401. e-mail peter.redden@signalgene.com.
    [†] SignalGene Inc., Guelph, Ontario, Canada.
    [‡] Present address: SYNX Pharma Inc. 6354 Viscount Road, Mississauga, ON, Canada L4V 1H3.
    [§] SignalGene Inc., Montreal, Quebec, Canada.

along with the indole analogues[17] (ERA-923 and TSE−424). These have estrogenic activity on skeletal and cardiovascular systems and are being developed as alternatives to estrogen-replacement therapy. On the other hand, ligands that have pure antiestrogenic activity on breast tissues are being developed for the treatment of breast cancer. These include faslodex and EM-800 (**4**) (although recently it has been suggested that EM-800 may possess more SERM-like activity than pure antiestrogenic activity[18,19]), which are currently in Phase II development.

Although generally these compounds display improved selectivity compared with tamoxifen, optimal tissue selectivity has not yet been demonstrated. As such there is still a need for additional diversity and new chemical scaffolds to allow for exploration of improved tissue selectivity. Here, we describe the discovery of a novel phenanthrene scaffold for estrogen receptor ligands utilizing a ligand based de novo design approach. We examined the activity of several members of this novel class in ER binding and cellular assays and the results demonstrate that this phenanthrene scaffold warrants further study as potential selective estrogen receptor modulators and/or pure antiestrogens.

Chemistry

De Novo Design. Our ligand based de novo design approach is based on the proprietary Evolutionary Molecular Design (EMD) computational technology.[20] Briefly, EMD utilizes structural information and biological activity of known pharmacologically active and inactive compounds as input structures to generate new structures that share and/or improve the biological activity of the original compounds (see Experimental Section).

For the present ER case, the steroidal compounds, estratriene, estratrien-17β-ol, estratriene-1,17β-diol, estradiol, estratriene-3,7β,17β-triol, 11-ketoestratriene-3,-17β-diol, estratriene-3-ol, 17-oxoestratriene-3-ol, 5α-androstane-3α,17β-diol, and progesterone, given in Figure 2, which are known to bind to ER[21] were used as input for the EMD process.

The first 40 molecules generated in the de novo design process were grouped into six structural classes or scaffolds. The first group contained structures, not surprisingly, based on estradiol. The second class consisted of the triphenylethylene skeleton, and the third class a series of flavanoid structures. The remaining three scaffolds were novel and not known in the estrogen literature. The result for one of these novel classes based on phenanthrene is described here. We will report on the other two scaffolds once synthesis and biological testing are complete which we believe will further demonstrate the utility and value of the EMD process.

Synthesis. The synthetic route for the preparation of the phenanthrene ligands is given in Scheme 1. Substituted anisoles are converted to *p*-methoxybenzaldehydes **5** by treatment with hydrogen chloride and zinc cyanide followed by aluminum trichloride. Aldol Condensation of **5** with *p*-methoxyacetophenone using potassium *tert*-butoxide, gave enones **6**. Treatment of **6** in a one-pot reaction with bromine, followed by addition of potassium acetate/acetic acid and then heating with
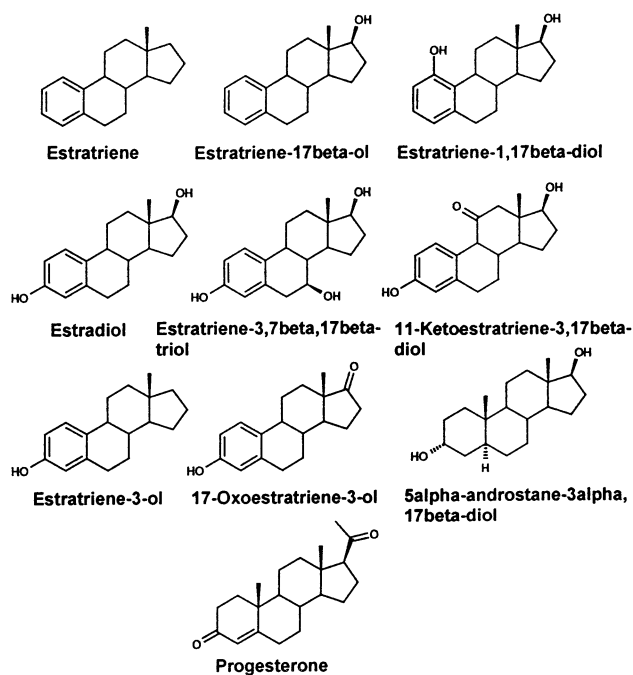

Figure 2. Steroids used as input for the de novo design approach, evolutionary molecular design (EMD).

DBU, gave ynones **7**. Heating **7** with 5-cyanopyrone[22] gave the biphenyl ketones **8**. Cyclization of **8** to give the key intermediate cyano phenanthrenes **9** occurred in a one-pot reaction by first bromination with NBS, followed by a Wittig reaction. Grignard treatment of **9** in the presence of a catalytic amount of cuprous bromide gave the keto phenanthrenes **10**, which were demethylated with either BBr$_3$ or concentrated hydrogen bromide in acetic acid to **11**. Treatment of **11** with 1-(2-chloroethyl)-piperidine gave a mixture of the mono- and disubstituted piperidine phenanthrenes with the desired phenanthrenes **12** isolated relatively easily. A second Grignard treatment of **12** generated the alcohol phenanthrenes **13**, which were converted to the alkenyl phenanthrenes **14**. Initial attempts at selective 9,10-double bond reduction of **14b** gave **15** using Pd/C hydrogenation conditions. However, Birch reduction of **12b** reduced the 9,10-double bond but also reduced the keto group to give the racemic 9,10-dihydrophenathrene **16**.

Computational Modeling. The crystal structure of ER$_\alpha$ only became available during the synthesis and biological testing of the molecules generated from the EMD process. Therefore, to gain further insight into the mode and energetics of binding of our de novo designed compounds, computational docking studies were conducted. The crystal structure used in the docking studies was that obtained from the cocrystallization of ER$_\alpha$ with raloxifene as found in the PDB database[23] (reference code: 1ERR). After removal of raloxifene from the pocket, ligands **12b**,**c**, **14b**,**c**, (1R)-**15**, (9R)-**17b**, (9S)-**17b**, and the four stereoisomers of **17a** were docked. For comparative purposes, raloxifene was also redocked using the same conditions as for all the other molecules.

Docking Results. The calculated binding energies from the docking experiments are presented in Table 1. The first column, $E_{bind,rigid}$, is the binding energy obtained with the rigid receptor approximation with the ligand having full torsional flexibility. The docking calculations utilize simulated annealing which optimizes

Scheme 1
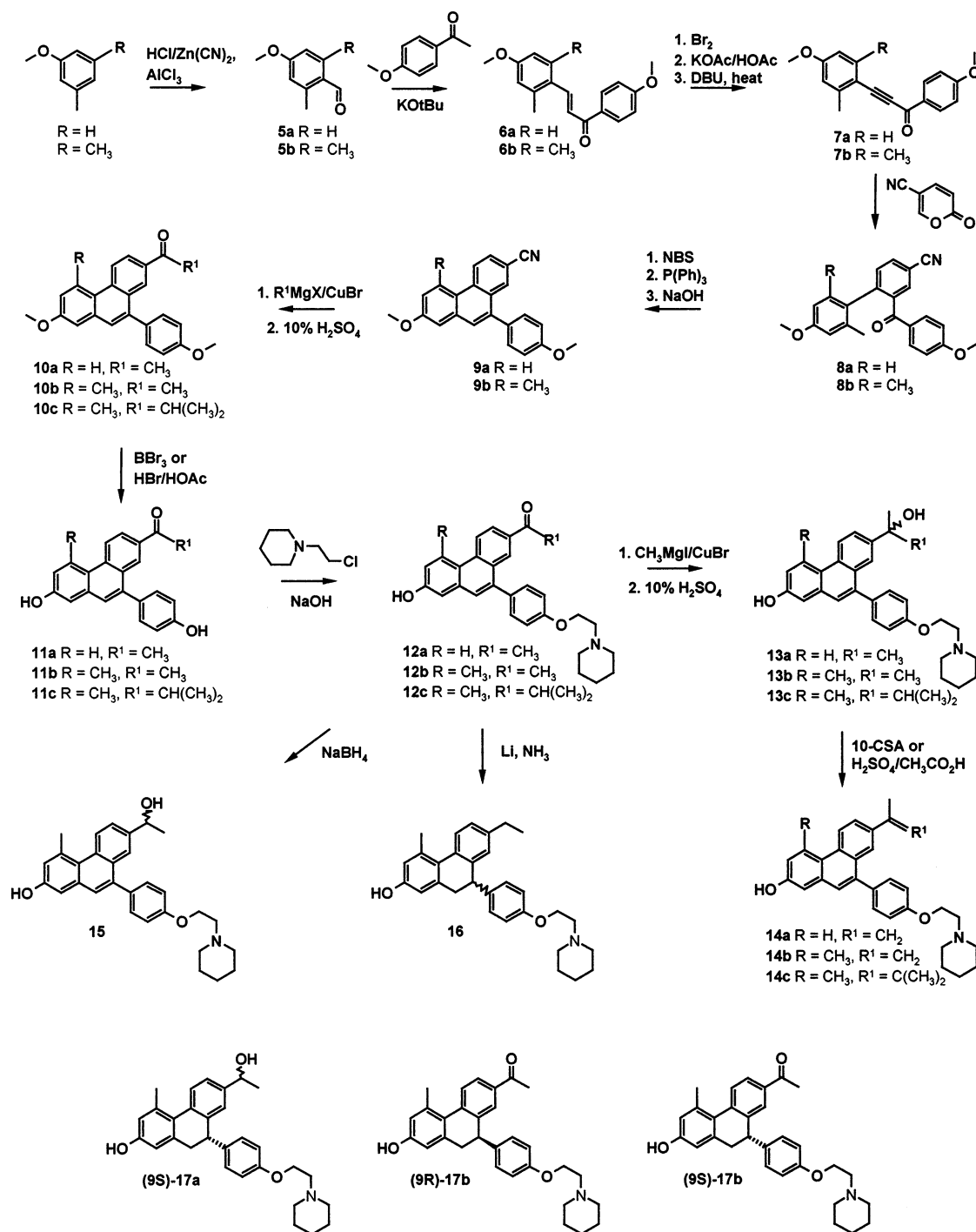
the torsion angles of the molecules in order to achieve optimum interaction with the receptor. In this process two important factors are neglected: potential changes in bond lengths during rotations around the torsion angles within the binding pocket and changes in the position of hydrogen atoms, such as sharing a hydrogen in hydrogen bonding. These effects have been incorporated and the results are also given in Table 1. $E_{bind,lig}$ gives the binding energy after a force field minimization of the ligand in the field of the receptor, while $E_{bind,H,lig}$ is the binding energy after a simultaneous optimization of the positions of the ligand and the surface hydrogen atoms. With all these approaches, the structure of the receptor is kept rigid and hence where an induced fit

would occur in reality, these calculations predict high binding energies. This can be remedied by keeping flexible both the ligand and the receptor atoms in the vicinity of the ligand. To avoid extreme distortion of the receptor structure, this was carried out in a stepwise fashion using a limited number of molecular mechanics steps (see Experimental Section). The results with 10 and 50 molecular mechanic (MM) steps are shown in columns $E_{bind,flex,10}$ and $E_{bind,flex,50}$. We limited the number of MM steps to 50 since a higher number of MM steps may lead to an unrealistic distortion of the receptor structure.

There are a number of assumptions that must be highlighted with respect to the results of these docking

Table 1. Results of the Docking Experiments with the Rigid and Flexible Receptor Approximations Using the ER_α Binding Site with Continuum Solvation (energies given in kcal/mol)

compound	$E_{bind,rigid}$[a]	$E_{bind,lig}$[b]	$E_{bind,H,lig}$[c]	$E_{bind,flex,10}$[d]	$E_{bind,flex,50}$[e]
14c	175.0	42.6	22.8	−12.6	−27.9
12c	156.3	14.5	−2.9	−29.1	−36.8
14b	54.4	−4.8	−8.2	−29.9	−41.6
12b	74.4	23.0	19.7	0.8	−2.9
(9R)-**17b**	66.3	−11.3	−14.8	−46.4	−43.1
(9S)-**17b**	34.7	−0.3	−5.3	−42.4	−46.5
(1R)-**15**	62.8	20.1	13.7	−13.2	−19.9
(1R,9R)-**17a**	49.8	14.0	8.5	−11.9	−17.7
(1S,9R)-**17a**	52.5	16.9	14.4	−14.8	−20.4
(1R,9S)-**17a**	26.5	−2.9	−15.5	−44.0	−40.8
(1S,9S)-**17a**	20.8	−14.8	−19.4	−52.0	−60.1
raloxifene	41.5	−25.8	−31.5	−53.6	−53.9

[a] The binding energy obtained with the rigid receptor approximation with the ligand having full torsional flexibility. [b] The binding energy after a force field minimization of the ligand in the field of the receptor. [c] The binding energy after a simultaneous optimization of the positions of the ligand and surface hydrogens. [d] To avoid extreme distortion of the receptor a limited number of molecular mechanic (MM) steps (10) were used. [e] 50 MM steps. See Experimental Section for further details.

experiments. Errors in the calculated binding energies are partly caused by the approximate nature of molecular mechanics energies and the treatment of solvation contributions. The continuum solvation terms may be unsuitable to describe the inside of the binding site and the effect of single water molecules in the pocket. Also, the position of bound water molecules might change from ligand to ligand but is fixed in the rigid receptor models. Although water molecules can move around in the flexible binding site model, this approximation greatly overemphasizes the flexibility of the receptor. The process is a minimization in Cartesian space and hence changes the position of both backbone and side chain protein atoms. However, since the receptor is very bulky, the backbone of the receptor cannot quickly assume conformations that are very different from the original conformation. However, despite the approximate nature of the calculated binding energies, the described docking studies provide additional evidence of the validity of our de novo designed structures with respect to binding at ER_α.

An examination of the docking results leads to some interesting observations. All protocols predict that raloxifene, **17a**, and **17b** bind better than any of the other molecules studied, while their relative order depends on the actual protocol used. The isopropyl ketone **12c** and alkene **14c** do not fare very well in the rigid receptor docking because of the conserved water molecule that is likely to be squeezed out in reality but was considered present in the docking studies presented in the table below. These, however, fit the pocket much better once the receptor within 10-Å of the ligand is fully relaxed. Apart from these, the ketone **12b** is predicted to be the worst binding molecule of all.

It is interesting to compare the predictions for the two stereoisomers of **17b**. With the rigid receptor approximation, the binding energy of (9R)-**17b** is higher than (9S)-**17b**. Unfortunately, neither of these ligands appears to bind in an optimal fashion. While (9R)-**17b** establishes a hydrogen bond in the tail section (with ASP351), its oxo-group is wedged into a hydrophobic region, unable to establish an H-bond with HIS524. (9S)-**17b** is slightly better in this rigid docking. Although
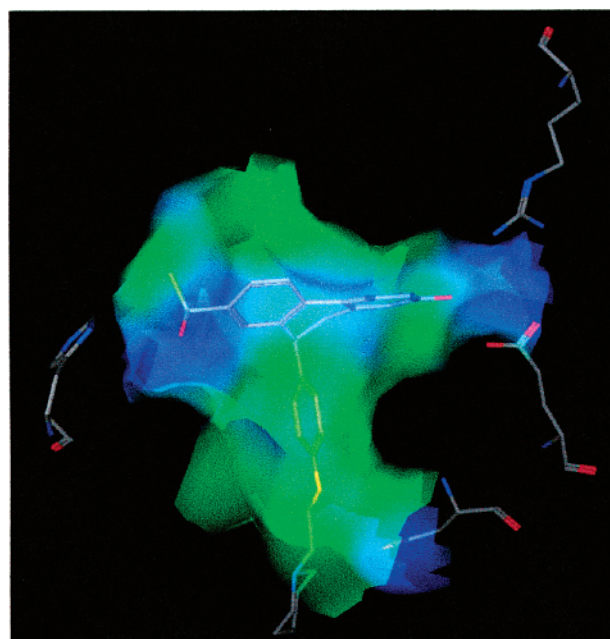
Figure 3. The Gauss-Conolly surface of the estrogen receptor (1ERR) binding pocket with docked (1S,9R)-**17a**. The surface is colored according to the hydrophobibicity of neighboring residues (green, hydrophobic; blue, hydrophilic). The residues nearest to the ligand are also shown (ARG392, GLU353, HIS524, and ASP351).

it cannot form any H-bond in the tail section due to steric restrictions and its oxo-group is also unable to H-bond to HIS524, the oxo-group is at least not forced close to a hydrophobic residue. However, if the ligand is relaxed, the predicted binding affinity of (9R)-**17b** becomes increasingly similar to (9S)-**17b** as the effect of the mismatch is reduced.

The comparison of the four different **17a** stereoisomers reveals the same trend. In all experiments (1S,9S)-**17a** is predicted to be the best stereoisomer, followed (1R,9S)-**17a**. The change in the stereochemistry of the 4-(2-(piperidin-1-yl)ethoxy)phenyl side chain appears to be critical, (1S,9R)-**17a** and (1R,9R)-**17a** are expected to be substantially less active. In these two cases the headgroup of the molecule is in a different binding mode to allow sufficient space for the side chain. Due to the fact that all four stereoisomers bind (albeit in different modes), experimentally these might compete with each other for binding to the receptor. The docked molecule, (1S,9S)-**17a**, is shown in Figure 3 where it nicely fits the pocket. It must be noted, however, that even the binding of (1S,9S)-**17a** is not perfect, as it is unable to hydrogen bond to HIS524.

Biology

Receptor Binding Assay. The binding data for compounds **12b,c**, **14b,c**, and **15** with human recombinant ER_α, and ER_β are given in Table 2. At ER_α the alcohol phenanthrene **15** gave a K_i of 120 nM, the alkene phenanthrenes **14b,c** gave 290 nM and 210 nM, respectively, and the ketones **12b,c** displayed lower binding (the K_i for **12c** was 490 nM). The 9,10-dihydrophenanthrene **16** was a more potent binder at ER_α (K_i of 8.69 nM) and showed a 20-fold selectivity for ER_α over ER_β.

Gene Transcription. Phenanthrenes **12b,c**, **14b,c**, and **15** and the dihydrophenanthrene **16** were evaluated

Table 2. Summary of In Vitro Activity of Phenanthrene Analogues

| compound | binding (K_i, nM)[a] | | transcriptional activation[b] |
	ER_α	ER_β	
12b	>1000	$630 + 47$	antagonist
12c	490 ± 130	>1000	antagonist
14b	290 ± 60	180 ± 17	antagonist
14c	210 ± 60	200 ± 10	antagonist
15	120 ± 54	190 ± 5	antagonist
16	8.69 ± 0.33	190 ± 35	antagonist
ICI 182780[c]	1.04 ± 0.91	1.39 ± 0.14	antagonist
4-OH-Tam[d]	0.25 ± 0.02	0.16 ± 0.04	partial agonist/ antagonist
DES[e]	0.49 ± 0.09	0.63 ± 0.13	agonist

[a] Binding affinity by competition with 0.5 nM [^{3}H]-17β-estradiolspecific binding to recombinant human estrogen receptors, ER_α and ER_β. Results represent the mean $\pm$ SEM of three separate experiments. [b] Effect on transcriptional potential (ERE-stimulated luciferase activity) of human ER_α and ER_β on the vitellogenin A2 ERE. [c] Pure antiestrogen. [d] 4-Hydroxytamoxifen. [e] Diethylstilbesterol.

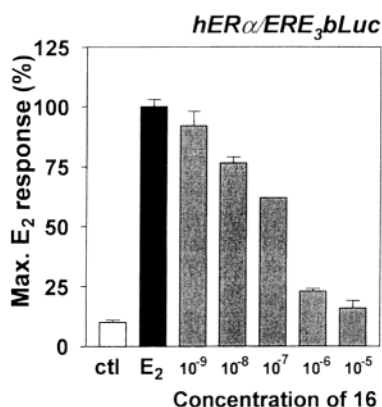**Figure 4.** Effect of **16** on ER_α-mediated transactivation. HepG2 cells were transfected with the pCMX-hER$_\alpha$ expression plasmid in the presence of the ERE$_3$bLuc reporter plasmid and treated with 10 nM E$_2$ in the absence or presence of increasing concentrations of **16** as indicated. Transfected cells treated with the vehicle (0.1% ethanol, control) indicate basal levels of transcription. Results represent the mean $\pm$ SEM of three separate experiments and are expressed as the percent of the maximun E$_2$ response in the absence of **16**.

in a gene transfection assay by monitoring the transcriptional activity of human ER_α on a luciferase reporter gene under the control of the vitellogenin A2 estrogen response element. As given in Table 2, all phenanthrenes were determined to be antagonists due to their ability to abrogate the E$_2$-responsive ER_α activity. As expected, DES was determined to be agonistic, and 4-hydroxytamoxifen was determined to be a partial agonist/antagonist. An example of the transcription assay result for **16** is shown in Figure 4.

MCF-7 Cell Proliferation Inhibition. The 9,10-dihydrophenanthrene **16** was tested for its ability to inhibit E$_2$-stimulated human breast cancer (MCF-7) cell proliferation. The result, shown in Figure 5, demonstrates that **16** effectively abrogates the E$_2$-stimulated cell growth.

Discussion

The identification of new chemical scaffolds that share or improve the biological activity of known drug target ligands is unquestionably of tremendous value in the drug discovery process. We have developed a novel
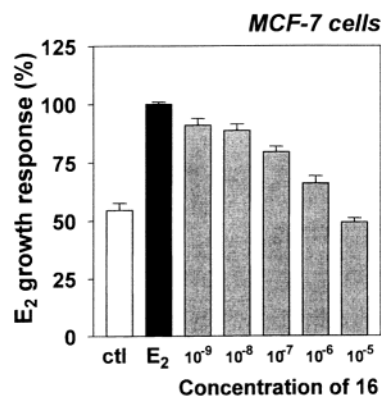

Figure 5. Effect of **16** on the inhibition of E$_2$-stimulated MCF-7 cell proliferation. Starved cells were treated with 10 nM E$_2$ in the absence or presence of increasing concentrations of **16** as indicated. The growth of unstimulated cells is shown (0.1% ethanol, control). Results represent the mean $\pm$ SEM of three separate experiments and are expressed as the percent of the maximun E$_2$ response in the absence of **16**.

proprietary ligand based computational technique, EMD, with the aim of doing exactly that. To demonstrate the utility of EMD, we chose ER (ER_α) as our first target since there is in fact a need for new chemical scaffolds and because the ER_α crystal structure (at the time) was unavailable. The steroids of Figure 2 were chosen as input structures. These steroids bind to ER_α with varying degrees of affinity irrespective of their agonistic/antagonistic profile. To incorporate only antagonistic activity, we incorporated the typical 4-(2-(piperidin-1-yl)ethoxy)phenyl side chain found in antiestrogens and SERMs.

As outlined in Scheme 1, the EMD-generated phenanthrene analogues were synthesized and subsequently tested for in vitro ER binding and antagonistic activity. The nanomolar binding of **12b**,**c**, **14b**,**c**, and **15** against human recombinant ER_α indicates that our ligand-based EMD de novo design approach was successful. This was particularly gratifying since the synthetic routes for these compounds, although straightforward, did require a number of steps.

Since 17-hydroxy-containing estradiol compounds were used as input (see Figure 1) and bind strongly to ER_α, not surprisingly H-bond donors (e.g., OH) on the C ring of the phenanthrene scaffold were generated (i.e., **15**). However, compounds containing H-bond acceptors (e.g., ketone) and hydrophobic (e.g., alkene) groups at this position, **12b** and **14b**, respectively, were also generated. Moreover, compounds **12c** and **14c** were also generated, indicating that there was a limited degree of bulk tolerance available in this C ring region. Once biological data became available, it was envisioned that subsequent design cycles using these compounds could further refine the requirements for this region if required. As it turned out, with the synthetic route devised, the conversion to all compounds was carried out very easily starting with the appropriate ketone intermediate (**10**, see Scheme 1).

As shown in Table 2, for the phenanthrene alcohol **15**, the binding was better at ER_α than for either the ketones **12b**,**c** or alkenes **14b**,**c**, although the differences are small. A related observation was seen for analogues of raloxifene where the ER binding was comparable when various groups including ethene replaced the 4'-

hydroxyl group.[24] Since **15** contains a secondary alcohol, as in estradiol, it might be expected to have higher binding than compounds with ketone or alkene functionality in this region. Moreover, since **15** is presumably a racemate, increased binding (2-fold maximum one enantiomer is not competing) might be seen with one of the individual enantiomers. These binding results tend to corroborate the computational predictions. Generally for both the rigid and flexible results (Table 2), the calculated binding of **15** (actually (1*R*)-**15**) is similar to the alkenes **14b**,**c** with the differences again being small. Of all the compounds **12b** was predicted to be the worst ligand at ER_α and did turn out to be the least active experimentally. Additionally, although we did not use ER_β in docking studies, **12b**, experimentally, was not a good binder at ER_β, being only slightly better than **12c**. **12c** was predicted to have binding similar to the alkenes **14b**,**c** but was somewhat less active experimentally.

Generally SERM or antiestrogenic compounds consist of a flat aromatic scaffold with either two phenolic groups[13] as is the case for raloxifene, its fixed ring analogues (**1**, LY335124 and **2**, LY357489), TSE-424, and EM652, as shown in Figure 1, or a single phenolic group and a phenyl group in place of the second phenol such as lasofoxifene (CP336,156) and levormeloxifene[25] plus a side-chain imparting antiestrogenicity. It has been suggested that it is the orientation of the basic amino-containing side chain of tamoxifen and raloxifene that is responsible for their different biological activities.[13]

With tamoxifen, the side chain is coplanar with the stilbene plane, giving rise to partial agonist/antagonist activity, whereas in raloxifene it is orthogonal with respect to the benzothiophene moiety conferring antagonism. Structurally related fixed ring analogues of raloxifene[13] (**1**, LY335124 and **2**, LY357489) and the benzopyran, EM-800, both which have orthogonal side chains, seem to corroborate this hypothesis. In particular it is the *S* configuration of EM-800 that appears to hold the biological activity.[18] Moreover, TSE-424, which is in clinical studies as a SERM for postmenopausal osteoporosis,[17] has the side chain orthogonal with the indole moiety.

Therefore, on the basis of the hypothesis regarding the amino-containing side chain geometry, the phenanthrene structures, having a coplanar 4-(2-(piperidin-1-yl)ethoxy)phenyl side chain, should behave more like tamoxifen than raloxifene with regards to antagonism. However, **12b**,**c**, **14b**,**c**, and **15** along with the pure antagonist ICI 182780 demonstrated only antagonist activity in the gene transfection assay. DES and 4-hydroxytamoxifen behaved as expected as an agonist and partial agonist/antagonist, respectively, in the assay. It is possible that any partial agonist/antagonist activity will only show up in uterine tissue, as was the case for *N*-arylbenzophenanthridines.[26]

Since an orthogonal side chain suggested antagonist activity we also considered the possibility that the 9,10-dihydrophenanthrenes as exemplified by **17a**,**b** would give antagonist activity. We chose the hypothetical compounds **17a**,**b** to dock since it was anticipated that these would be the compounds that would be generated from **12b**. Since these compounds contain four

and two stereoisomers, respectively, each required separate docking. Our computational docking studies using the ER_α crystal structure (cocrystallized with raloxifene) suggests that it is the 9*S* as opposed to the 9*R* configuration of the 4-(2-(piperidin-1-yl)ethoxy)-phenyl side chain of these 9,10-dihydrophenanthrenes that docks with higher binding to ER_α. For instance for both the rigid and flexible docking experiments, both **17a** and **17b** with the side chain in the *S* configuration are predicted to dock with greater affinity than with the side chain in the *R* configuration. Also **17a** and **17b** with the side chain in the *S* configuration were predicted to bind better to ER_α than any of the aromatic phenanthrenes. However, our initial attempt to generate either **17a** or **17b** from **12b** resulted in both the reduction of the ketone as well as the 9,10 double bond to give the alkyl 9,10-dihydrophenanthrene **16**. Although **16** is presumably a racemic mixture, it was a substantially more potent ER binder than the phenanthrenes (see Table 2). This was gratifying since, although we did not study **16** computationally, this experimental result indirectly corroborates our computational studies regarding the 9,10-dihydrophenanthrenes. **16** also displayed only antagonistic activity and was effective at inhibiting E_2 stimulated MCF-7 cell proliferation. Clearly, additional agonist/antagonist profiling of **16** and other 9,10-dihydrophenanthrene analogues as well as the separation of the enantiomers is required to fully explore this scaffold for an anti-estrogen/SERM indication.

In summary, a series of analogues based on the phenanthrene scaffold were identified using our proprietary EMD de novo design method. After synthesis and testing, all compounds with the exception of **12b** demonstrated affinity for ER_α as well as ER_β. **12b**,**c**, **14b**,**c**, and **15** did not show any agonistic activity in the gene transcription assay, which is very encouraging in the quest for alternate antiestrogenic or SERM-like compounds. The 9,10-dihydrophenanthrene **16** demonstrated even higher affinity for ER than the phenanthrenes, was antagonistic, and inhibited E_2-stimulated MCF-7 cell growth. Overall this experimental in vitro evidence suggests that the de novo designed phenanthrene (as well as the 9,10-dihydrophenanthrene) scaffold analogues are worthy of further study as antiestrogens or SERMs and is the first example that demonstrates the utility of our EMD approach.

Experimental Methods

Computational Modeling. Ligand docking was performed with full torsional flexibility of the ligands into both a rigid receptor and a flexible receptor using algorithms within the MOE suite along with algorithms developed during the course of this work. In all calculations the Born continuum solvation model was applied[27−29] in assessing solvation−desolvation with a constant (distance independent) dipole term, as implemented in the Molecular Operating Environment (MOE) suite of programs.[30]

Flexible Docking of Molecules into a Rigid Receptor. The docking algorithm utilized was a multiple start Monte Carlo method.[31,32] First, a box is defined around the ligand, such that it is sufficiently large to encompass the active site fully but small enough to prevent docking on the receptor surface. In the docking process different orientations and conformations of the ligand are tested, in which all of its atoms are inside the docking box. Each docking run begins with the ligand in a random conformation and orientation. Some or all

of the rotatable bonds of the ligand are then randomly perturbed, while the bond lengths are held fixed. The energy of a given configuration is evaluated using the Merck force field (MMFF94), using the terms described below. Although calculating force field energies for docking purposes is not widely used due to lengthy computer time, the accuracy of the method has been demonstrated.[33,34] Each step is evaluated and is accepted or rejected on the basis of the Metropolis criterion.[35] Favorable binding modes are generated in repeated simulated annealing runs. A simulated annealing run consists of a sequence of Monte Carlo cycles: the ligand temperature within each cycle is kept constant but is systematically reduced from one cycle to the next (in our case, 1000 to 100 K in six cycles). This simulated annealing process is repeated a number of times, leading to different docked orientations and conformations. In all cases, at least 100 such configurations were produced.

The potential changes in bond lengths during rotations around the torsion angles were taken into account by the optimization of ligand geometry, shown as column $E_{\text{bind,lig}}$ in Table 1. To account for the changes in the position of hydrogen atoms as a result of hydrogen bonding the positions of surface hydrogens were also optimized (shown as $E_{\text{bind,lig,H}}$ in Table 1). Only those hydrogens were considered that were within 3 Å of any of the ligand atoms. The 3-Å radius ensures that only four residues (i.e., ARG394, GLU353, ASP351, and HIS524) of ER_α directly interacting with the ligand and the preserved water molecule are affected. In both cases, the optimizations were terminated after 50 molecular mechanics steps, and it was made sure in all cases that the calculations were sufficiently close to convergence.

Approximating the Flexibility of the Receptor. The starting points for the 'flexible receptor' experiments were those orientations and conformations that were already docked into the rigid ER_α binding site from above. Previously a partial receptor flexibility protocol has been described.[36] In this procedure, those residues that contained atoms within 10 Å of the ligand were optimized first, while the ligand itself and the rest of the protein were held fixed. Next, the geometry of the ligand was optimized, followed by the optimization of both the ligand and the 10-Å vicinity of the binding site. In our case, the docking calculations in MOE apply simulated annealing, and this process optimizes the torsion angles of the molecules in order to achieve optimum interaction with the receptor. As described above, the changes in bond lengths of the ligand and the position of hydrogen atoms are also important to consider. In view of this fact, it was thought to be unwise to consider the receptor atoms first, since the ligand is usually much more easily deformed than the receptor. Hence, the protocol was changed in such a way that first the ligand position was optimized, followed by the neighboring site and then finally the ligand and the neighboring site together. This modified protocol leads to substantially lower energies with the same number of optimization steps than the reference.[36] All minimizations were performed using the MMFF94 force field[37] with the Born continuum solvation model. Technically this is not the same as docking ligands into a flexible binding site, since the receptor structure was not being optimized while the best conformation and orientation of the ligand were sought. However, as this procedure was undertaken for all low energy conformations/orientations of the ligand, it is likely that the found solutions would correspond to those obtained from a docking process to a flexible receptor. Both 10 and 50 were tested as the number of MM steps in the optimization of receptor atom positions. The interaction radius of receptor atoms considered around the ligand was 10 Å.

The Calculation of Binding Energy. As described above, the calculated binding energy is obtained from the full force field energy of the docked molecule and the receptor, including solvation contribution. Only residues that have atoms within 10-Å of the ligand were taken into account in the energy calculations. The energy balance for the binding process is calculated assuming the following single-step process:

$$\text{ligand} + \text{substrate} \rightarrow \text{complex}$$

From this, the nonbonded ligand−receptor interaction energy, E_{bind}, is calculated as follows:

$$E_{\text{bind}} = E^{\text{cpx}} - (E^{\text{lig}} + E^{\text{prot}}) \tag{1}$$

where the E denotes the total energies with the superscripts corresponding to the complex, the ligand and the protein, respectively. The energy terms can be partitioned into bonding (subscript bd) and nonbonding (subscript nb) terms:

$$E_{\text{bind}} = [E_{\text{nb}}^{\text{cpx}} - (E_{\text{nb}}^{\text{lig}} + E_{\text{nb}}^{\text{prot}})] + [E_{\text{bd}}^{\text{cpx}} - (E_{\text{bd}}^{\text{lig}} + E_{\text{bd}}^{\text{prot}})] \tag{2}$$

To perform the docking calculations fast, the energy is referenced to the energy of the ligand in the geometry it is found in the complex ($E^{\text{lig,cpxgeom}}$). This is different from the actual lowest energy conformer by a constant term (ΔE^{lig}). The bonding and nonbonding terms can then be expressed as follows:

$$E_{\text{nb}}^{\text{lig}} = E_{\text{nb}}^{\text{lig,cpxgeom}} + (E_{\text{nb}}^{\text{lig}} - E_{\text{nb}}^{\text{lig,cpxgeom}}) = E_{\text{nb}}^{\text{lig,cpxgeom}} + \Delta E_{\text{nb}}^{\text{lig}} \tag{3}$$

$$E_{\text{bd}}^{\text{lig}} = E_{\text{bd}}^{\text{lig,cpxgeom}} + (E_{\text{bd}}^{\text{lig}} - E_{\text{bd}}^{\text{lig,cpxgeom}}) = E_{\text{bd}}^{\text{lig,cpxgeom}} + \Delta E_{\text{bd}}^{\text{lig}} \tag{4}$$

From equations 2−4, the binding energy is:

$$E_{\text{bind}} = [E_{\text{nb}}^{\text{cpx}} - (E_{\text{nb}}^{\text{lig,cpxgeom}} + E_{\text{nb}}^{\text{prot}})] - \Delta E_{\text{nb}}^{\text{lig}} + [E_{\text{bd}}^{\text{cpx}} - (E_{\text{bd}}^{\text{lig,cpxgeom}} + E_{\text{bd}}^{\text{prot}})] - \Delta E_{\text{bd}}^{\text{lig}} \tag{5}$$

The first square bracket is calculated as the total interaction energy, E_{int}. The second square bracket is zero as a result of the rigid receptor approximation. From this, the following formula can be derived:

$$E_{\text{bind}} = E_{\{\text{int}\}} + E^{\text{lig,cpxgeom}} - (\Delta E^{\text{lig}} - E^{\text{lig,cpxgeom}}) = E_{\{\text{int}\}} + E^{\text{lig,cpxgeom}} - E^{\text{lig}} \tag{6}$$

Here the first two terms are obtained directly from the force field calculations. The third term, the bonded internal energy of the unbound ligand (E^{lig}), was calculated from a stochastic conformational search[38] using continuum solvation (100 failures in a row, using a 7-kcal/mol energy window).

When comparing binding energies in the table, it must also be born in mind that the experimentally measurable quantity is the free energy of binding that would also include entropic terms. No attempts have been made here to allow for entropic contributions, although it is likely that the studied ligands would have similar entropic contributions. Obviously, all of the calculated binding energies must be viewed as approximations at different levels of accuracy to the true binding energy. The rigid receptor approximation entirely neglects induced fit effects, while the flexible receptor approximation at the MM = 50 steps, $r = 10$ Å grossly overestimates them. It is likely that at the time-scale of the binding event the receptor shape cannot change extensively, and therefore it is expected that the true binding energy should lie somewhere between the rigid and flexible receptor values.

Competitive Binding. The human ER_α and ER_β proteins were in vitro transcribed−translated using the rabbit reticulocyte lysate (Promega, Madison, WI) with pCMX-hER$_\alpha$ and pCMX-hER$_\beta$ templates, respectively, as previously described.[39] K_is were calculated using Prism (Graphpad Software, Inc.). The cDNAs encoding the full length ERs were generous gifts from Dr. V. Giguère, McGill University Health Center.

Cell Culture, DNA Transfection, and Luciferase Assay. For transient transfections, Cos-1 and HepG2 cells (ATCC, Manassas, VA) were seeded in 12-well plates in phenol red-free DMEM supplemented with 10% charcoal-treated FBS, 100 μg/mL penicillin, and 100 μg/mL streptomycin. At 50−75% confluence, cells were transfected with 1.0 μg of luciferase reporter plasmid, 0.1 μg of receptor expression plasmid, and

0.5 μg of pCMX-β-galactosidase expression plasmid using the Polyfect reagent as described by the manufacturer (Qiagen Inc., Mississauga, ON). Cell treatment, lysis, and assays for luciferase and β-galactosidase were as described previously.[39] Values were expressed as arbitrary light units normalized to the β-galactosidase activity of each sample.

Breast Cancer Cell Growth Inhibition. MCF-7 cells (ATCC, Manassas, VA) were seeded in 48-well plates in Iscove's phenol red-free medium containing 10% FBS and 10 μg/mL insulin. The next day, the cells were starved for 72 h in medium containing 10% dextran-coated charcoal treated serum in the absence of insulin. The cells were treated with 10 nM E$_2$ in the absence or presence of increasing concentrations of **16**. Cell number was determined after 96 h using the MTS assay as described by the manufacturer (Promega, Madison, WI).

Evolutionary Molecular Design (EMD). Briefly, EMD utilizes structural information and biological activity of known pharmacologically active compounds as input structures to generate new structures that share and/or improve the biological activity of the original compounds. This process takes place in two stages.

The first stage of the design process begins with the construction of virtual receptors (VRs) that identify the structural features of ligands, which are required for binding to specific biological receptors. These VRs act as computational mimics of their biological counterparts and are mathematical objects and not molecular models of the biological binding site. As VRs are constructed, features that are essential for high binding affinity are identified including location and type of functional groups, requirements for appropriate solvation effects, and space filling properties. VRs are created through an iterative process using structural and biological data from known active and inactive compounds. These compounds comprise a training set that is used to optimize the ability of the VR to mimic the binding properties of a corresponding biological receptor. Each VR is represented by a unique string of characters that encodes a complex three-dimensional surface. Accurate estimates of binding affinities between the VR surface and the members of the training set are rapidly calculated using pairwise contributions to molecular interactions including solvation effects, electrostatic interactions, and induced fitting of flexible ligands, as well as entropic effects. The calculated binding affinity is compared to the experimental values for the members in the training set to obtain an initial threshold fitness score. The VRs that meet this initial criterion are then further mutated and recombined to give optimized VRs that must be able to reproduce the experimental binding free energies with a predetermined quality.

In the second stage of the EMD process, information obtained from the VRs is used in a de novo design process (called a molecular assembler) to generate new structures. These new structures must fit into the VR and hence satisfy the identified requirements for biological activity as determined from the training set. Using an iterative procedure, the strings corresponding to the proposed ligands are subjected to mutations and crossovers, till the designs satisfy the predetermined fitness score. These designed molecules are subjected to retrosynthetic analysis to quantify their synthetic feasibility and their physicochemical properties (e.g., logP, pK_a) are evaluated using computational approaches prior to selection for synthesis. Further details on the method have been given elsewhere.[20]

Synthesis. 4-Methoxy-2-methylbenzaldehyde (5a). 3-Methylanisole (36.6 g, 300 mmol) was reacted as described for **5b** to give 41.8 g (93%) of **5a**. ^{1}H NMR (400 MHz, CDCl$_3$) δ_H 2.65 (3H, s, CH$_3$), 3.87 (3H, s, OCH$_3$), 6.74 (1H, d, ArH), 6.85 (1H, dd, ArH), 7.76 (1H, d, ArH), 10.11 (1H, s, CHO).

4-Methoxy-2,6-dimethylbenzaldehyde (5b). 3,5-Dimethylanisole (25.3 g, 0.186 mol) was added to (CHCl$_2$)$_2$ (180 mL)

and maintained at 17 °C. Zn(CN)$_2$ (37.1 g, 0.316 mol) was added, and HCl gas was bubbled through the mixture with stirring. The rate of HCl gas addition was adjusted to allow for HCl absorption. After 1 h of HCl gas addition, the rate of absorption significantly decreased and AlCl$_3$ (37.2 g, 0.279 mol) was added. A slow rate of HCl gas flow was maintained. The temperature was increased to 55 °C and the reaction maintained at this temperature for 3 h. The reaction mixture was then poured onto a mixture of ice (800 mL) and concentrated HCl (800 mL). The content of the reaction vessel was then rinsed twice with CHCl$_3$ (200 mL) and added to the aqueous layer. The resulting biphasic layer was stirred at 60−65 °C overnight. The organic layer was separated and the aqueous layer washed with 200 mL and 150 mL of the organic layer. The combined extract was washed with deionized water (3 × 200 mL), and the organic solvents were removed by evaporation. The concentrate was transferred to a distillation flask equipped with a Vigreux column and distilled at 110 °C (0.7 mmHg) to give a distillate (29.2 g) containing residual (CHCl$_2$)$_2$ and a 2:1 mixture of the desired 4-methoxy-2,6-dimethylbenzaldehyde and 6-methoxy-2,4-dimethylbenzaldehyde isomer. The distillate was added to methyl *tert*-butyl ether and crystallized overnight at 4 °C. The crystals were filtered and washed with 5 mL of a mixture of ethyl acetate:hexane (1:12) to give 7.84 g of **5b**. The mother liquor was concentrated and chromatographed on silica gel with ethyl acetate/hexane (1:12) to give an additional 10.74 g (18.58 g total, 61%). ^{1}H NMR (400 MHz, CDCl$_3$) δ_H 2.62 (6H, s, CH$_3$), 6.59 (2H, s, ArH), 10.48 (1H, s, CHO).

3-(4-Methoxy-2-methylphenyl)-1-(4-methoxyphenyl)-propenone (6a). **5a** (41.8 g, 279 mmol) was reacted as described for **6b** to give 51 g (65%) of **6a**. ^{1}H NMR (400 MHz, CDCl$_3$) δ_H 2.48 (3H, s, CH$_3$), 3.85 (3H, s, OCH$_3$), 3.90 (3H, s, OCH$_3$), 6.76−6.82 (2H, s, ArH), 6.99 (2H, d, ArH), 7.40, (1H, d, COCH), 7.70 (1H, d, ArH), 8.08 (1H, d, ArCH),8.50 (2H, d, ArH).

3-(4-Methoxy-2,6-dimethylphenyl)-1-(4-methoxyphenyl)-propenone (6b). Compound **5b** (18.58 g, 0.113 mol) and 4-methoxyacetophenone (17.42 g, 0.116 mol) were added to anhydrous ethanol (110 mL) and NaOH (2.5 g) and stirred overnight at room temperature. The precipitate that formed was filtered, washed with water (3 × 50 mL), and dried overnight under high vacuum to give 29.75 g of **6b**. The filtrate was stirred overnight to give an additional 1.1 g (30.85 g, 92%). ^{1}H NMR (400 MHz, CDCl$_3$) δ_H 2.44 (6H, s, CH$_3$), 3.83 (3H, s, OCH$_3$), 3.90 (3H, s, OCH$_3$), 6.66 (2H, s, ArH), 6.99 (2H, d, ArH), 7.16, (1H, d, ArCH), 7.96 (1H, d, COCH), 8.01 (2H, d, ArH).

3-(4-Methoxy-2-methylphenyl)-1-(4-methoxyphenyl)-propynone (7a). (i) 2,3-Dibromo-3-(4-methoxy-2-methylphenyl)-1-(4-methoxyphenyl)propan-1-one. **6a** (51.0 g, 182 mmol) was reacted as described for **7b**, step i, to give 2,3-dibromo-3-(4-methoxy-2-methylphenyl)-1-(4-methoxyphenyl)-propan-1-one that was used without further purification. ^{1}H NMR (400 MHz, CDCl$_3$) δ_H 2.48 (3H, s, CH$_3$), 3.84 (3H, s, OCH$_3$), 3.92 (3H, s, OCH$_3$), 5.90 (1H, d, ArCHBr), 6.00 (1H, d, COCHBr), 6.74 (1H, d, ArH), 6.88 (1H, dd, ArH), 7.03 (2H, d, ArH), 7.54 (1H, d, ArH), 8.07 (2H, d, ArH).

(ii) Acetic Acid, 2-Bromo-1-(4-methoxy-2-methylphenyl)-3-(4-methoxyphenyl)-3-oxopropyl Ester. Crude 2,3-dibromo-3-(4-methoxy-2-methylphenyl)-1-(4-methoxyphenyl)-propan-1-one was reacted as described for **7b**, step ii, to give 79 g of acetic acid, 2-bromo-1-(4-methoxy-2-methylphenyl-)-3-(4-methoxyphenyl)-3-oxopropyl ester that was used without further purification. ^{1}H NMR (400 MHz, CDCl$_3$) δ_H 1.88 (3H, s, COCH$_3$), 2.60 (3H, s, CH$_3$), 3.81 (3H, s, OCH$_3$), 3.91 (3H, s, OCH$_3$), 5.36 (1H, d, COCHBr), 6.60 (1H, d, COCHAr), 6.36 (1H, d, ArH), 6.81 (1H, dd, ArH), 7.00 (2H, d, ArH), 7.35 (1H, d, ArH), 8.05 (2H, d, ArH).

(iii) 3-(4-Methoxy-2-methylphenyl)-1-(4-methoxyphenyl)propynone (7a). Crude acetic acid, 2-bromo-1-(4-methoxy-2-methylphenyl)-3-(4-methoxyphenyl)-3-oxopropyl ester was reacted as described for **7b**, step iii, to give 13 g (26%) of **7a**. ^{1}H NMR (400 MHz, CDCl$_3$) δ_H 2.59 (3H, s, CH$_3$), 3.85 (3H, s, OCH$_3$), 3.91 (3H, s, OCH$_3$), 6.82−8.21 (7H, ArH).

3-(4-Methoxy-2,6-dimethylphenyl)-1-(4-methoxyphenyl)-propynone (7b). (i) 2,3-Dibromo-3-(4-methoxy-2,6-dimethylphenyl)-1-(4-methoxyphenyl)propan-1-one. To a solution of **6b** (30.9 g, 104 mmol), dissolved in CH_2Cl_2 (200 mL) and cooled in an ice bath, was added a solution of Br_2 (16.7 g, 5.37 mL, 104 mmol) in CH_2Cl_2 (100 mL) over 105 min with additional stirring for 2 h. A second portion of Br_2 (1.2 mL) in CH_2Cl_2 (50 mL) was added over 30 min and the reaction left at room-temperature overnight, followed by the evaporation of the solvent to give 2,3-dibromo-3-(4-methoxy-2,6-dimethylphenyl)-1-(4-methoxyphenyl)propan-1-one that was used without further purification. ^{1}H NMR (400 MHz, $CDCl_3$) δ_H 2.51 (3H, s, CH_3), 2.71 (3H, s, CH_3), 3.81 (3H, s, OCH_3), 3.92 (3H, s, OCH_3), 6.16 (1H, d, COCHBr), 6.24 (1H, d, ArH), 6.34 (1H, d, ArCHBr), 6.66 (1H, d, ArH), 7.03 (2H, d, ArH), 8.07 (2H, d, ArH).

(ii) Acetic Acid, 2-Bromo-1-(4-methoxy-2,6-dimethylphenyl-)-3-(4-methoxyphenyl)-3-oxopropyl Ester. Crude 2,3-dibromo-3-(4-methoxy-2,6-dimethylphenyl)-1-(4-methoxyphenyl)propan-1-one from step i was added to acetic acid (550 mL) and KOAc (12.5 g, 130 mmol) and stirred for 6 h. Additional KOAc (3.0 g) was added and the mixture stirred overnight. The HOAc was evaporated and the residue dissolved in water (300 mL) and extracted with $CHCl_3$ (300 mL), and the $CHCl_3$ extract was washed with water (3 × 150 mL) and concentrated to give acetic acid, 2-bromo-1-(4-methoxy-2,6-dimethylphenyl)-3-(4-methoxyphenyl)-3-oxopropyl ester that was used without further purification. ^{1}H NMR (400 MHz, $CDCl_3$) δ_H 1.88 (3H, s, COCH₃), 2.58 (3H, s, CH₃), 2.65 (3H, s, CH₃), 3.80 (3H, s, OCH₃), 3.91 (3H, s, OCH₃), 5.76 (1H, d, COCHBr), 6.60 (2H, s, ArH), 6.87 (1H, d, ArCHO), 6.66 (1H, d, ArH), 7.02 (2H, d, ArH), 8.04 (2H, d, ArH).

(iii) 3-(4-Methoxy-2,6-dimethylphenyl)-1-(4-methoxyphenyl)propynone (7b). DBU 36.2 g, 238 mmol) and crude acetic acid, 2-bromo-1-(4-methoxy-2,6-dimethylphenyl)-3-(4-methoxyphenyl)-3-oxopropyl ester from step ii were added to THF (350 mL) and heated to 55 °C overnight. The reaction mixture was filtered and the precipitate washed with THF (2 × 100 mL). The filtrate was evaporated and the residue dissolved in $CHCl_3$ (300 mL) and washed with water (2 × 150 mL), 8% HCl (pH 2, 150 mL), and water (2 × 150 mL). It was noted that the final separation was made easier if an aqueous solution of $NaHCO_3$ (15 mL) was added to the last extraction. After evaporation of the solvent and drying overnight under high vacuum, the crude material was crystallized from anhydrous toluene (30 mL) by cooling to room temperature and then to 4 °C to give 22.4 g, (73%) of **7b**. ^{1}H NMR (400 MHz, $CDCl_3$) δ_H 2.55 (6H, s, CH_3), 3.82 (3H, s, OCH_3), 3.89 (3H, s, OCH_3), 6.65−8.22 (6H, ArH).

4′-Methoxy-2′-methyl-2-(4-methoxybenzoyl)biphenyl-4-carbonitrile (8a). 7a (5.61 g, 20.0 mmol) was reacted as described for 8b to give 8a in quantitative yield. ^{1}H NMR (400 MHz, $CDCl_3$) δ_H 2.14 (3H, s, CH_3), 3.74 (3H, s, OCH_3), 3.84 (3H, s, OCH_3), 6.56−7.79 (10H, ArH).

4′-Methoxy-2′,6′-dimethyl-2-(4-methoxybenzoyl)biphenyl-4-carbonitrile (8b). 7b (4.20 g, 15.7 mmol) and 4-cyanopyrone[22] (1.90 g, 15.7 mmol) were heated at 190 °C for 17 h. The crude reaction was chromatographed on silica gel with ethyl acetate/hexane (1:6) then ethyl acetate/hexane (1:2) to give 4.4 g (75%) of **8b**. ^{1}H NMR (400 MHz, $CDCl_3$) δ_H 1.96 (6H, s, CH_3), 3.75 (3H, s, OCH_3), 3.88 (3H, s, OCH_3), 6.54−7.83 (9H, ArH).

7-Methoxy-10-(4-methoxyphenyl)phenanthrene-2-carbonitrile (9a). (i) 2′-Bromomethyl-2-(4-methoxybenzoyl)biphenyl-4-carbonitrile. 8a (4.6 g, 13 mmol) was reacted as described for **9b**, step i, to give 2′-bromomethyl-2-(4-methoxybenzoyl)biphenyl-4-carbonitrile that was used without further purification.

(ii) 5-Methoxy-2-[2′-(4-methoxybenzoyl)-4′-cyanophenyl]benzyltriphenylphosphonium Bromide. Crude 2′-bromomethyl-2-(4-methoxybenzoyl)biphenyl-4-carbonitrile was reacted as described for **9b**, step ii, to give 5-methoxy-2-[2′-(4-methoxybenzoyl)-4′-cyanophenyl]benzyltriphenylphosphonium bromide that was used without further purification.

(iii) 7-Methoxy-10-(4-methoxyphenyl)phenanthrene-2-carbonitrile. Crude 5-methoxy-2-[2′-(4-methoxybenzoyl)-4′-cyanophenyl]benzyltriphenylphosphonium bromide was reacted as described for **9b**, step iii, to give 2.8 g 64% of **9a**. ^{1}H NMR (400 MHz, $CDCl_3$) δ_H 3.94 (3H, s, OCH_3), 3.99 (3H, s, OCH_3), 7.08−8.73 (11H, ArH).

7-Methoxy-10-(4-methoxyphenyl)-5-methylphenanthrene-2-carbonitrile (9b). (i) 6′-Methyl-2′-bromomethyl-2-(4-methoxybenzoyl)biphenyl-4-carbonitrile. To a refluxing solution of **8b** (45.5 g, 122 mmol) and AIBN (1.0 g) in CCl_4 (2.5 L) was added a mixture of NBS (23.0 g, 129 mmol) and AIBN (1.0 g) in 10 equal portions. The reaction was refluxed for 2 h after the addition of the last portion of NBS/AIBN. The mixture was concentrated to approximately 1 L and washed three times with water (1 L). The organic layer was dried with anhydrous Na_2SO_4 and filtered and the solvent removed. Toluene (200 mL) was added to the residue and then evaporated. Repeating this procedure gave 48 g of 6′-methyl-2′-bromomethyl-2-(4-methoxybenzoyl)biphenyl-4-carbonitrile that was used without further purification.

(ii) 5-Methoxy-2-[2′-(4-methoxybenzoyl)-4′-cyanophenyl]-(3-methylbenzyl)triphenylphosphonium Bromide. The crude 6′-methyl-2′-bromomethyl-2-(4-methoxybenzoyl)-biphenyl-4-carbonitrile from step i was dissolved in DMF (200 mL), triphenyphosphine (48 g) added, and the reaction stirred at 100 °C for 5 h. The hot reaction was slowly poured into vigorously stirring methyl *tert*-butyl ether (4 L) and then stirred for an additional 30 min and filtered. The crude 5-methoxy-2-[2′-(4-methoxybenzoyl)-4′-cyanophenyl]-(3-methylbenzyl)triphenylphosphonium bromide was washed twice with methyl *tert*-butyl ether (200 mL) and immediately dissolved in CH_2Cl_2 (1 L).

(iii) 7-Methoxy-10-(4-methoxyphenyl)-5-methylphenanthrene-2-carbonitrile (9b). The crude 5-methoxy-2-[2′-(4-methoxybenzoyl)-4′-cyanophenyl]-(3-methylbenzyl)triphenylphosphonium bromide from step ii was added over 5 h to a vigorously stirred mixture of CH_2Cl_2 (2 L) and 50% aqueous NaOH (1 L) at 35 °C. Stirring was continued for an additional 3 h at 35−40 °C. The organic layer was separated and washed consecutively with 1 N HCl (200 mL), water (200 mL), and saturated $NaHCO_3$ (200 mL). After drying the organic layer over anhydrous Na_2SO_4 and removing the solvent, the residue was crystallized from CH_2Cl_2/hexanes/ethanol (80/60/10, 150 mL) to give 24 g of **9b**. The filtrated was concentrated and chromatographed on silica using CH_2Cl_2/hexanes (50/50) to give an additional 5.5 g (total 29.5 g, 68.5%). ^{1}H NMR (400 MHz, $CDCl_3$) δ_H 3.12 (3H, s, CH_3), 3.94 (3H, s, OCH_3), 3.97 (3H, s, OCH_3), 7.07−8.94 (10H, ArH).

1-[7-Methoxy-10-(4-methoxyphenyl)phenanthren-2-yl]ethanone (10a). 9a (2.8 g, 8.3 mmol) and methylmagnesium bromide (3 M) in diethyl ether (6.1 mL, 18 mmol) were reacted as described for **10b** to give **10a**. ^{1}H NMR (400 MHz, $CDCl_3$) δ_H 2.61 (3H, s, COCH₃) 3.94 (3H, s, OCH_3), 3.99 (3H, s, OCH_3), 7.07−8.73 (11H, ArH).

1-[7-Methoxy-10-(4-methoxyphenyl)-5-methylphenanthren-2-yl]ethanone (10b). Following the procedure outlined for **10c**, compound **9b** (1.22 g, 3.46 mmol) and methylmagnesium bromide (3 M) in diethyl ether (2.5 mL) were reacted to give 1.42 g of **10b** in quantitative yield. ^{1}H NMR (400 MHz, $CDCl_3$) δ_H 2.61 (3H, s, CH_3), 3.15 (3H, s, COCH₃), 3.94 (3H, s, OCH_3), 3.97 (3H, s, OCH_3), 7.08−8.94 (10H, ArH).

1-[7-Methoxy-10-(4-methoxyphenyl)-5-methylphenanthren-2-yl]-2-methylpropan-1-one (10c). 9b (10.0 g, 28.3 mmol) was added to anhydrous THF (200 mL), and isopropylmagnesium chloride (2.0 M) in THF (15.6 mL) was added with stirring under Ar. After 10 min, crystalline CuBr (72 mg) was added, and the reaction stirred for 9 h. TLC analysis indicated that there was still starting material present, and an additional 8 mL of the Grignard reagent was added and the reaction stirred overnight. To the reaction was added 10% H_2SO_4 (150 mL), and the mixture was placed on a rotary evaporator to remove the THF. The remaining aqueous layer was stirred overnight at room temperature then extracted with $CHCl_3$ (3 × 250 mL), washed with water (3 × 150 mL). After

removing the CHCl₃, the residue was dried under high vacuum to give 11.2 g (quantitative yield) of **10c**. ¹H NMR (400 MHz, CDCl₃) δ_H 1.22 (6H, d, CH₃), 3.15 (3H, s, CH₃), 3.54 (1H, septet, COCH), 3.94 (3H, s, OCH₃), 3.96 (3H, s, OCH₃), 7.09−8.93 (10H, ArH).

1-[7-Hydroxy-10-(4-hydroxyphenyl)phenanthren-2-yl]-ethanone (11a). **10a** was reacted as described for **11b** to give **11a**. ¹H NMR (400 MHz, DMSO-d_6) δ_H 2.59 (3H, s, COCH₃), 6.95−8.87 (11H, ArH), 9.7 (1H, br s, OH), 10.1 (1H, br s, OH).

1-[7-Hydroxy-10-(4-hydroxyphenyl)-5-methylphenan-thren-2-yl]ethanone (11b). BBr₃ (100 mL, 1 M in CH₂Cl₂) was added to **10b** (6.76 g, 18.3 mmol) in CH₂Cl₂ (200 mL) at −70 to − 60 °C. The reaction was stirred overnight at −60 to 3 °C and then poured into water/ice (500 mL) and extracted with CHCl₃/acetone (2.5 L, 5/1). After the solvent was evaporated, the residue was chromatographed on silica gel using a gradient of ethyl acetate:methanol (95:5) to ethyl acetate: methanol (80:20) to give **11b**. ¹H NMR (400 MHz, DMSO-d_6) δ_H 2.16 (3H, s, CH₃), 2.67 (3H, s, COCH₃), 6.52−8.48 (10H, ArH), 8.81 (1H, br s, OH), 9.91 (1H, br s, OH).

1-[7-Hydroxy-10-(4-hydroxyphenyl)-5-methylphenan-thren-2-yl]-2-methylpropan-1-one (11c). **10c** (5.53 g, 13.9 mmol), 48% HBr (44 mL), and acetic acid (55 mL) were heated (oil bath at 126 °C) in a closed thick-walled pressure flask for 3.5 h. The reaction was then poured into water (300 mL), extracted with ethyl acetate (3 × 250 mL), and washed with water (3 × 150 mL). After the solvent was removed, the residue was dried under high vacuum to yield **11c** quantitatively. ¹H NMR (400 MHz, DMSO-d_6) δ_H 1.10 (6H, d, CH₃), 3.03 (3H, s, CH₃), 3.56 (1H, septet, COCH), 6.96−8.87 (10H, ArH), 9.65 (1H, br s, OH), 10.1 (1H, br s, OH).

1-{7-Hydroxy-10-[4-(2-(piperidin-1-yl)ethoxy)phenyl]-phenanthren-7-yl}ethanone (12a). **11a** (1.35 g, 4.12 mmol) was reacted as described for **12b** to give 0.175 g (9.7%) of **12a**. ¹H NMR (400 MHz, DMSO-d_6) δ_H 1.40 (2H, br s, NCH₂-CH₂CH_2), 1.53 (4H, m, NCH₂CH_2CH₂), 2.49 (4H, br s, NCH_2-CH₂CH₂), 2.57 (3H, s, CH₃), 2.70 (2H, t, OCH₂CH_2N), 4.16 (2H, t, OCH_2CH₂N), 7.11−8.86 (11H, ArH), 10.12 (1H, br s, OH).

1-{7-Hydroxy-5-methyl-10-[4-(2-(piperidin-1-yl)ethoxy)-phenyl]phenanthren-2-yl}ethanone (12b). **11b** (0.135 g, 0.394 mmol) was dissolved in anhydrous DMF (5 mL). NaH (75 mg, 60% in oil) was added and the reaction stirred for 10 min. at room temperature. A solution of 1-(2-chloroethyl)-piperidine hydrochloride (75 mg, 0.40 mmol) in DMF (4.5 mL) was added slowly over 2 h. After the addition was complete, the reaction was stirred for 2 h at 40−50 °C then overnight at room temperature. The reaction mixture was added to water (50 mL), extracted with ethyl acetate (75 mL), dried, concentrated, and chromatographed on silica using ethyl acetate: methanol (9:1) to give **12b**. ¹H NMR (400 MHz, CDCl₃) δ_H 1.53 (2H, br s, NCH₂CH₂CH_2), 1.76 (4H, m, NCH₂CH_2CH₂), 2.51 (3H, s, COCH₃), 2.72 (4H, br s, NCH_2CH₂CH₂), 2.93 (2H, t, OCH₂CH_2N), 3.10 (3H, s, CH₃), 4.24 (2H, t, OCH_2CH₂N), 6.83−8.87 (10H, ArH). Anal. C₃₀H₃₁NO₃ (C, H, N).

1-{7-Hydroxy-5-methyl-10-[4-(2-(piperidin-1-yl)ethoxy)-phenyl]phenanthren-7-yl}-2-methylpropan-1-one (12c). **11c** (1.1 g, 3.0 mmol), Aliquat (3.03 g, 7.5 mmol), NaOH (1.2 g, 30 mmol), and 1-(2-chloroethyl)piperidinium hydrochloride (0.552 g, 3.0 mmol) were added to TMU (70 mL) and heated at 50 °C for 11 h. The reaction was added to water (500 mL), acidified with concentrated HCl (3 mL), and then neutralized with an excess of NaHCO₃ until pH 8. The reaction was extracted with ethyl acetate (3 × 250 mL), and the combined extracts were washed with water (2 × 150 mL) and then concentrated. The residue was chromatographed on silica gel with acetone/hexane (1:2) to give 0.383 g (26.5%) of **12c**. ¹H NMR (400 MHz, CDCl₃) δ_H 1.15 (6H, d, CH₃), 1.53 (2H, br s, NCH₂CH₂CH_2), 1.75 (4H, m, NCH₂CH_2CH₂), 2.71 (4H, br s, NCH_2CH₂CH₂), 2.92 (2H, t, OCH₂CH_2N), 3.07 (3H, s, CH₃), 3.44 (1H, septet, COCH), 4.23 (2H, t, OCH_2CH₂N), 6.83−8.88 (10H, ArH). Anal. C₃₂H₃₅NO₃ (C, H, N).

(+)-7-(1-Hydroxy-1-methylethyl)-4-methyl-9-[4-(2-(pi-peridin-1-yl)ethoxy)phenyl]phenanthren-2-ol (13b). **12b** (0.65 g, 1.4 mmol) in anhydrous THF (150 mL) was cooled to 0 °C. Methylmagnesium bromide (3 M) in diethyl ether (4.8 mL, 14 mmol) was added. The reaction was stirred overnight at 0 °C then cold 1 N HCl (35 mL) was added. Ethyl acetate (100 mL) was added and the aqueous phase saturated with Na₂CO₃. The organic layer was separated and dried and the solvent removed to yield a yellow, glassy residue (0.83 g) of **13b** that was used without further purification.

(+)-7-(1-Hydroxy-1,2-dimethylpropyl)-4-methyl-9-[4-(2-(piperidin-1-yl)ethoxy)phenyl]phenanthren-2-ol (13c). **12c** (0.570 g, 1.2 mmol) and methylmagnesium iodide (3 N) in THF (3.0 mL) was added and the mixture stirred overnight at room temperature. After the THF was removed, CHCl₃ (50 mL) was added to the residue along with H₂SO₄ (0.675 g) dissolved in water (20 mL, pH 1). The residue completely dissolved. Excess NaHCO₃ was added and the organic layer separated, evaporated, and dried under high vacuum to give **13c** in quantitative yield. ¹H NMR (400 MHz, CDCl₃) δ_H 0.77 (3H, d, CH₃), 0.83 (3H, d, CH₃), 1.47 (3H, s, CH₃), 1.53 (2H, m, NCH₂CH₂CH_2), 1.72 (4H, m, NCH₂CH_2CH₂), 2.01 (1H, septet, CH(CH₃)₂), 2.67 (4H, br s, NCH_2CH₂CH₂), 2.90 (2H, t, OCH₂CH_2N), 3.09 (3H, s, CH₃), 4.21 (2H, t, OCH_2CH₂N), 6.88−8.80 (10H, ArH).

7-Isopropenyl-4-methyl-9-[4-(2-(piperidin-1-yl)ethoxy)-phenyl]phenanthren-2-ol (14b). Crude **13b** was dissolved in CH₂Cl₂ (20 mL), 10-camphorsulfonic acid (1 g) was added, and the mixture was refluxed for 1 h. After the solvent was removed, the residue was dissolved in ethyl acetate (100 mL), a saturated solution of Na₂CO₃ (25 mL) was added, and the mixture was stirred for 15 min. The organic layer was separated, dried, and concentrated and the residue chromatographed on silica gel using hexanes:acetone (60:40) to yield 0.412 g (65%) of **14b**. ¹H NMR (400 MHz, CDCl₃) δ_H 1.52 (2H, br s, NCH₂CH₂CH_2), 1.75 (4H, m, NCH₂CH_2CH₂), 2.05 (3H, s, CH₃), 2.71 (4H, br s, NCH_2CH₂CH₂), 2.92 (2H, t, OCH₂CH_2N), 3.10 (3H, s, CH₃), 4.24 (2H, t, OCH_2CH₂N), 5.05 (1H, s, =CH), 5.36 (1H, s, =CH), 6.84−8.78 (10H, ArH). Anal. C₃₁H₃₃NO₂ (C, H, N).

7-(1,2-Dimethylpropenyl)-4-methyl-9-[4-(2-(piperidin-1-yl)ethoxy)phenyl]phenanthren-2-ol (14c). **13c** (0.587 g, 1.2 mmol) was dissolved in glacial acetic acid (7.0 mL), and concentrated H₂SO₄ (1 drop) was added. The mixture was heated for 20 min at 75 °C with stirring. The reaction was neutralized with NaHCO₃ (10.5 g in 25 mL of water) and extracted with methyl *tert*-butyl ether (3 × 25 mL), evaporated, and dried under high vacuum. The residue was chromato-graphed on silica gel with acetone/hexane (1:2) to give 0.407 g (85%) of **14c**. ¹H NMR (400 MHz, CDCl₃) δ_H 0.77 (3H, d, CH₃), 0.83 (3H, d, CH₃), 1.47 (3H, s, CH₃), 1.55 (2H, m, NCH₂-CH₂CH_2), 1.76 (4H, m, NCH₂CH_2CH₂), 2.72 (4H, br s, NCH_2-CH₂CH₂), 2.95 (2H, t, OCH₂CH_2N), 3.11 (3H, s, CH₃), 4.24 (2H, t, OCH_2CH₂N), 6.87−8.78 (10H, ArH). Anal. C₃₃H₃₇NO₂ (C, H, N).

(+)-7-(1-Hydroxyethyl)-4-methyl-9-[4-(2-(piperidin-1-yl)ethoxy)phenyl]phenanthren-2-ol (15). **12b** (0.550 g, 1.2 mmol) was dissolved in methanol (45 mL). NaBH₄ (0.175 g, 4 equiv) was added in portions over 1 h at −5 to −3 °C. The reaction was brought to room temperature and stirred for 2 h. The solvent was removed, and water and ethyl acetate were added. The mixture was acidified with concentrated HCl to pH 2, and then excess Na₂CO₃ was added. The organic layer was separated and the aqueous layer extracted with ethyl acetate. The combined organic layers were washed with brine, dried, and concentrated. The residue was chromatographed on silica with hexanes:acetone (1:1) to yield 0.447 g, 81%) of **15**. ¹H NMR (400 MHz, DMSO-d_6) δ_H 1.34 (3H, d, CH₃), 1.40 (2H, m, NCH₂CH₂CH_2), 1.52 (4H, m, NCH₂CH_2CH₂), 2.47 (3H, s, CH₃), 2.47 (4H, br s, NCH_2CH₂CH₂), 2.71 (2H, t, OCH₂CH_2N), 3.01 (3H, s, CH₃), 4.16 (2H, t, OCH_2CH₂N), 4.79 (1H, dq, CH), 5.19 (1H, d, OH), 7.05−8.76 (10H, ArH), 9.75 (1H, s, OH).

(+)-7-Ethyl-4-methyl-9-[4-(2-(piperidin-1-yl)ethoxy)-phenyl]phenanthren-2-ol (16). **12b** (0.091 g, 0.2 mmol) was

dissolved in dry THF (5 mL). Liquid NH_3 (6 mL) was added via a cannula at -78 °C. Li (4 mg) was then added and the reaction stirred for 30 min. Additional Li (10 mg) was added, and the reaction stirred for an additional 1 h. The reaction was quenched with solid NH_4Cl (3.3 g). The NH_3 was allowed to boil off and the residue partitioned between CH_2Cl_2 and water. The water layer was separated and extracted with CH_2-Cl_2, and the combined organic layers were dried, concentrated, and chromatographed on silica using a gradient of methanol:CH_2Cl_2 (5:95 to 30:70) to give 0.035 g (40%) of **16**. ^{1}H NMR (400 MHz, $CDCl_3$) δ_H 1.16 (3H, t, CH_3), 1.47 (2H, m, NCH_2-CH_2CH_2), 1.67 (4H, m, $NCH_2CH_2CH_2$), 2.54 (2H, q, CH_2), 2.55 (3H, s, CH_3), 2.56 (4H, br s, $NCH_2CH_2CH_2$), 2.82 (2H, t, OCH_2CH_2N), 2.87 (1H, dd, ArCH), 3.00 (1H, dd, ArCH) 3.92 (1H, dd, ArCHAr), 4.10 (2H, m, OCH_2CH_2N), 6.50–7.56 (9H, ArH). Anal. $C_{30}H_{35}NO_2$ (C, H, N).

References

(1) Carson-Jurica, M. A.; Schrader, W. T.; O'Malley, B. W. Steroid Receptor Family: Structure and Functions. *Endocrinol. Rev.* **1990**, *11*, 201–220.

(2) Jordan, V. C. Studies on the Estrogen Receptor in Breast Cancer – 20 Years as a Target for the Treatment and Prevention of Breast Cancer. *Breast Cancer Res. Treat.* **1995**, *36*, 267–285.

(3) Gradishar, W. J.; Jordan, V. C. Clinical Potential of New Antiestrogens. *J. Clin. Oncol.* **1997**, *15*, 840–852.

(4) Jordan, V. C. Molecular Mechanisms of Antiestrogen Action in Breast Cancer. *Breast Cancer Res. Treat.* **1994**, *31*, 41–52.

(5) Mitlak, B. H.; Cohen, F. J. In Search of Optimal Long-Term Female Hormone Replacement: The Potential of Selective Estrogen Receptor Modulators. *Horm. Res.* **1997**, *48*, 155–163.

(6) Smith, C. L.; O'Malley, B. W. Evolving Concepts of Selective Estrogen Receptor Action: From Basic Science to Clinical Applications. *Trends Endocrinol. Metab.* **1999**, *10*, 299–300.

(7) McDonnell, D. P. The Molecular Pharmacology of SERMs. *Trends Endocrinol. Metab.* **1999**, *10*, 301–311.

(8) MacGregor, J.; Jordan, V. G. Basic Guide to the Mechanism of Antiestrogen Action. *Pharmacol. Rev.* **1998**, *50*, 151–196.

(9) Mosselman, S.; Polman, P.; Dijkema, R. ER beta: Identification and Characterization of a Novel Human Estrogen Receptor. *FEBS Lett.* **1996**, *392*, 49–53.

(10) Hall, J. M.; McDonnell, D. P. The Estrogen Receptor beta-Isoform (ERbeta) of the Human Estrogen Receptor Modulates ERalpha Transcriptional Activity and is a Key Regulator of the Cellular Response to Estrogens and Antiestrogens. *Endocrinology* **1999**, *140*, 5566–5578.

(11) Pennisi, E. Differing Roles Found for Estrogen's Two Receptors. *Mol. Endocrinol.* **1997**, *277*, 1439–1510.

(12) Mitlak, B. H.; Cohen, F. J. Selective Estrogen Receptor Modulators: A Look Ahead. *Drugs* **1999**, *57*, 653–663.

(13) Grese, T. A.; Pennington, J. P.; Sluka, J. P.; Adrian, M. D.; Cole, H. W.; Fuson, T. R.; Magee, D. E.; Phillips, D. L.; Rowley, E. R.; Shetler, P. K.; Short, L. L.; Venugopalan, M.; Yang, N. N.; Sato, M.; Blasebrook, A. L.; Bryant, H. U. Synthesis and Pharmacology of Conformationally Restricted Raloxifene Analogues: Highly Potent Selective Estrogen Receptor Modulators. *J. Med. Chem.* **1998**, *41*, 1272–1283.

(14) Black, L. J.; Jones, C. D.; Falcone, J. F. Antagonism of Estrogen Action with a New Benzothiophene Derived Antiestrogen. *Life Sci.* **1983**, *28*, 1031–1036.

(15) Foster, A. B.; Jarman, M.; Leung, O. T.; McCague, R.; Leclercq, G.; Devleeschouwer, N. Hydroxy Derivatives of Tamoxifen. *J. Med. Chem.* **1985**, *28*, 1491–1497.

(16) Chander, S. K.; McCague, R.; Luqmani, Y.; Newton, C.; Dowsett, M.; Jarman, M.; Coombes, R. C. Pyrrolidino-4-Iodotamoxifen and 4-Iodotamoxifen, New Analogues of the Antiestrogen Tamoxifen for the Treatment of Breast Cancer. *Cancer Res.* **1991**, *51*, 5851–5858.

(17) Miller, C. P.; Collini, M. D.; Tran, B. D.; Harris, H. A.; Kharode, Y. P.; Marzolf, J. T.; Moran, R. A.; Henderson, R. A.; Bender, R. H. W.; Unwalla, R. J.; Greenberger, L. M.; Yaardley, J. P.; Abou-Gharbia, M. A.; Lyttle, C. R.; Komm, B. S. Design, synthesis and Preclinical Characterization of Novel, Highly Selective Indole Estrogens. *J. Med. Chem.* **2001** *44*, 1654–1657.

(18) Gauthier, S.; Caron, B.; Cloutier, J.; Dory, Y. L.; Favre, A.; Larouche, D.; Mailhot, J.; Ouellet, C.; Schwerdtfeger, A.; Le-blanc, G.; Martel, C.; Simard, J.; Merand, Y.; Belanger, A.; Labrie, C.; Labrie, F. (*S*)-(+)-4-[7-(2,2-dimethyl-1-oxopropoxy)-4-methyl-2-[4-[2-(1-piperidinyl)-ethoxy]phenyl]-2H-1-benzopyran-3-yl]-phenyl-2,2-dimethylpropanoate (EM-800): A Highly Potent, Specific, and Orally Active Nonsteroidal Antiestrogen. *J. Med. Chem.* **1997**, *40*, 2117–2122.

(19) Labrie, F.; Labrie, C.; Belanger, A.; Simard, J.; Gauthier, S.; Luu-The, V.; Merand, Y.; Giguere, V.; Candas, B.; Luo, S.; Martel, C.; Singh, S. M.; Fournier, M.; Coquet, A.; Richard, V.; Charbonneau, R.; Charpenet, G.; Tremblay, A.; Tremblay, G.; Cusan, L.; Veilleux, R. EM-652 (SCH 57068), a Third Generation SERM Acting as Pure Antiestrogen in the Mammary Gland and Endometrium. *J. Steroid Biochem. Mol. Biol.* **1999**, *69*, 51–84.

(20) Schmidt, J. M., University of Guelph, US Patent 5699268, 1995.

(21) Wiese, T. E.; Polin, L. A.; Palomino, E. and Brooks, S. K. Induction of the Estrogen Specific Response of MCF-7 Cells by Selected Analogues of Estradiol-17β: A 3D QSAR Study. *J. Med. Chem.* **1997**, *40*, 3659–3669.

(22) Kvita, V.; Sauter, H. The Synthesis of Some 2H–Pyran-2-one Derivatives. *Helv. Chim. Acta* **1990**, *73*, 883.

(23) Berman, H. M.; Westbrook, J.; Feng, Z.; Gilliland, G.; Bhat, T. N.; Weissig, H.; Shindyalov, I. N.; Bourne, P. E. The Protein Data Bank. *Nucl. Acid Res.* **2000**, *28*, 235–242.

(24) Grese, T. A.; Cho, S.; Finley, D. R.; Godfrey, A. G.; Jones, C. D.; Lugar, C. W., III; Martin, M. J.; Matsumoto, K.; Pennington, L. D.; Winter, M. A.; Adrian, M. Dee; Cole, H. W.; Magee, D. E.; Phillips, D. Lynn; Rowley, E. R.; Short, L. L.; Glasebrook, A. L.; Bryant, H. U. Structure–Activity Relationships of Selective Estrogen Receptor Modulators: Modifications to the 2-Arylben-zothiophene Core of Raloxifene. *J. Med. Chem.* **1997**, *40*, 146–167.

(25) Sata, M.; Grese, T. A.; Dodge, J. A.; Bryant, H. U.; Turner, C. H. Emerging Therapies for the Prevention or Treatment of Postmenopausal Osteoporosis. *J. Med. Chem.* **1999**, *42*, 1–24.

(26) Grese, T. A.; Adrian, M. Dee; Phillips, D. Lynn; Shelter, P. K.; Short, L. L.; Glasebrook, A. L.; Bryant, H. U. Photochemical Synthesis of *N*-Arylbenzophenanthridine Selective Estrogen Modulators (SERMs). *J. Med. Chem.* **2001**, *44*, 2857–2860.

(27) Still, W. C.; Tempczyk, A.; Hawley, R. C.; Hendrickson, T. Semianalytical Treatment of Solvation for Molecular Mechanics and Dynanmics. *J. Am. Chem. Soc.* **1990**, *112*, 6127–6129.

(28) Qiu, D.; Shenkin, S.; Hollinger, F. P.; Still, W. C. The GB/SA Continuum Model for Solvation. A Fast Analytical Method for the Calculation of Approximate Born Radii. *J. Phys. Chem. A* **1997**, *101*, 3005–3014.

(29) Schaefer, M.; Karplus, M. A. Comprehensive Analytical Treatment of Continuum Electrostatics. *J. Phys. Chem.* **1996**, *100*, 1578–1599.

(30) Molecular Operating Environment, Version 2001.01. Chemical Computing Group Inc., Montreal, Quebec, Canada. (http://www.chemcomp.com).

(31) Hart, T. N.; Read, R. J. A Multiple-Start Monte Carlo Docking Method. *PROTEINS: Struct. Func. Genet.* **1992**, *13*, 206–222.

(32) Morris, G. M.; Goodsell, D. S.; Huey, R.; Olsen, A. J. Distributed automated docking of flexible ligands to proteins: Parallel applications of AutoDock 2.4. *J. Comput. Aided Mol. Design.* **1996**, *10*, 293–304.

(33) Holloway, M. K.; Wai, J. M.; Halgren, T. A.; Fitzgerald, P. M. D.; Vacca, J. P.; Dorsey, B. D.; Levin, R. B.; Thompson, W. J.; Chen, L. J.; deSolms, S. J.; Gaffin, N.; Ghosh, A. K.; Giuliani, E. A.; Graham, S. L.; Guare, J. P.; Hungate, R. W.; Lyle, T. A.; Sanders, W. M.; Tucker, T. J.; Wiggins, M.; Wiscount, C. M.; Woltersdorf, O. W.; Young, S. D.; Darke, P. L. and Zugay, J. A. A Priori Prediction of Activity for HIV-1 Protease Inhibitors Employing Energy Minimization in the Active Site. *J. Med. Chem.* **1995**, *38*, 305–317.

(34) Shen, J.; Pearlstein, R. A.; Vaz, R. J.; Kominos, D.; Effland, R. C. The Use of Interaction Energy and Solvation Entropy to Rank Order Docked Ligand-Protein Complexes for Lead Optimization: Application to Thermolysin Inhibitors. *Med. Chem. Res.* **1999**, *9*, 501–512.

(35) Metropolis, N.; Rosenbluth, A. W.; Rosenbluth, M. N.; Teller, A. H. Equation of State Calculations by Fast Computing Machines. *J. Chem. Phys.* **1953**, *21*, 1087–1092.

(36) Fink, B. E.; Mortensen, D. S.; Stauffer, S. R.; Aron, Z. D.; Katzenellenbogen, J. A. Research Paper-Novel Structural Tem-plates for Estrogen-Receptor Ligands and Prospects for Combi-natorial Synthesis of Estrogens. *Chem. Biol.* **1999**, *6*, 205–219.

(37) Halgren, T. A. The Merck Molecular Force Field. 1. Basis, Form, Scope, Parametrization, and Performance of MMFF94. *J. Com-put. Chem.* **1996**, *17*, 490–519.

(38) Ferguson, D. M.; Raber, D. J. A New Approach to Probing Conformational Space with Molecular Mechanics: Random Incremental Pulse Search. *J. Am. Chem. Soc.* **1989**, *111*, 4371–4378.

(39) Tremblay, A.; Tremblay, G. B.; Labrie, C.; Labrie, F.; and Giguere, V. EM-800, a Novel Antiestrogen, Acts as a Pure Antagonist of the Transcriptional Functions of Estrogen Recep-tors α and β. *Endocrinology* **1998**, *139*, 111–118.